Evaluating Human Electromagnetic Exposure in a UAV-aided Network

Thomas Detemmerman

Supervisor(s): Prof. dr. ir. Wout Joseph, Prof. dr. ir. Luc Martens

Abstract—Society relies more than ever on the availability of wireless networks. Due to the mobility of a UAV, a UAV-aided network is able to provide this necessary access in case the existing terrestrial network gets damaged. However, the public is concerned about the potential health effects of the electromagnetic radiation caused by these networks. Therefore, mobile devices and base stations have to comply to strict legislation enforced by the government.

This research investigates how different scenarios influence power consumption, electromagnetic exposure and specific absorption rate. These different scenarios are defined by various flying heights, number of UAVs available and population sizes. Also, the proper microstrip patch antenna is defined and attached to the UAV. The antenna will be responsible for the communication between the UAV and the users it covers. Its performance is compared to an equivalent isotropic radiator. Thereafter, the network will be optimized towards goals like electromagnetic exposure of the average user or power consumption of the entire network; which results in conflicting requirements.

To accomplish this goal, the capacity based deployment tool of the WAVES research group at Ghent University will be extended so it would be able to calculate electromagnetic exposure. Further, the tool now also provides support to optimize the networks towards electromagnetic exposure or power consumption.

It looks from the results that the microstrip patch antenna with an aperture angle of 90° is a suitable starting point for an antenna. This directional antenna focusses electromagnetic radiation where it is needed. Unwanted sideways radiation is therefore reduced by design. The sufficiently large aperture angle covers enough users. The antenna is recommended to be deployed in a power consumption optimized network since less Unmanned Aerial Vehicle (UAV)s are required and therefore also less expensive. The optimal flying height for the city centre of Ghent is believed to be situated at 80 metres since lower flying heights require much more UABSs and higher flying heights have a negative influence on the electromagnetic exposure.

Keywords—Deployment tool, Electromagnetic exposure, LTE Microstrip patch antenna, Power consumption, Radiation pattern, Specific absorption rate (SAR), UAV, Unmanned aerial base stations Wireless access network, Emergency network

I. Introduction

SOCIETY is constantly getting more and more dependent on wireless communication. On any given moment, in any given location, an electronic device can request to connect to the bigger network, starting from small Internet of Things (IoT) up to self-driving cars.

Also in exceptional and possibly life threatening situations, the public relies on the cellular network despite the fact that the network might be severely damaged and not properly functioning anymore. One solution for a fast temporarily deployable back-up network is to use UAVs. A base station can be attached to these flying UAVs to support the network over a limited area. This approach is also useful in case of an unexpected increase in traffic. For example during the terrorist attacks at Brussels Airport, mobile network operators saw all telecommunications drastically increasing causing moments of contention. Some operators even decided to temporarily exceed the exposure limits in order to handle all connections [1]. Electromagnetic exposure caused by these networks can however not be neglected. Research shows how excessive electromagnetic radiation can cause diverse biological side effects [2], [3]. It becomes clear that electromagnetic exposure is a key value when designing a UAV-aided network and should definitely not surpass the limits predefined by the government.

UAV-aided networks can, thanks to their mobility, easily be repositioned towards a certain goal. Several papers explain how a network can be optimized towards different goals like power consumption. However, very limited research has been done where a UAV-aided network is optimized towards electromagnetic exposure. While several publications exist, discussing how the electromagnetic exposure can be calculated, most of them only consider a limited number of sources; e.g. only base stations or only the user's mobile device. Papers who cover electromagnetic exposure from all the different sources and convert it into a single value are rather limited.

This research proposes a method to optimize the network towards electromagnetic exposure and power consumption when considering all four sources of radiation in a telecommunications network, being: the user's own phone, the base station that is serving this user, all devices from other users in the network and all other active base stations that are not serving this user. In this way, the contribution of each source towards the total electromagnetic exposure can easily be identified.

The behaviour of the electromagnetic exposure and power consumption of the network will be analysed by applying the tool in different scenarios by using different types of antennae, various flying height and population densities. Values like Specific Absorption Rate (SAR), electromagnetic exposure and power consumption will give insight in how the network behaves so the network could be optimized accordingly.

To make this research possible, an existing capacity based deployment tool developed by the WAVES research group at Ghent University is extended for the specific purpose. This planning tool describes a fully configured UAV-network which is a suitable starting point for this research.

II. State of the Art

A. Electromagnetic exposure

Users in a telecommunication network are exposed to various sources of electromagnetic radiation, expressed in

V/m. Once the exposure is absorbed by the human body, we speak of the specific absorption rate (SAR) which is expressed in W/kg. The International Commission on Non-Ionizing Radiation Protection (ICNIRP) has concluded that the threshold effect for SAR^{wb}_{10g} is at 4 W/kg meaning that any higher absorption rate would overwhelm the thermoregulatory capacity of the human body [4], [5]. All these values are subjected to limitations enforced by the government. This research is based in Ghent, a Flemish city in Belgium where an individual antenna in the 2.6 GHz frequency band could not exceed 4.5 V/m and the cumulative sum of all fixed sources has its maximum at 31 V/m [4], [6]. The maximum whole body SAR-values for a mobile device over a 10 g tissue (SAR_{10g}) is defined at $0.08W/kg$ [7], [4], [8]. The Federal Communications Commission (FCC) of the United States of America (USA) follows the recommendations of the Institute of Electrical and Electronics Engineers (IEEE) Std C95.1-1999 [9], [10] that defines regulations based on 1 g tissue. The SAR^{wb}_{1g} is therefore defined at 1.6 W/kg despite the fact that this value has been reviewed and changed by the IEEE to 8 W/kg in Std C95.1-2005 [10]. An overview is given in table I.

Description	Value	Units
SAR^{wb}_{10g} (ICNIRP)	4	W/kg
SAR^{wb}_{10g} for base station(BE)	0.08	W/kg
SAR^{head}_{10g} for UE (BE)	2	W/kg
SAR^{head}_{1g} for UE (USA)	1.6	W/kg

TABLE I: Overview of the different SAR limitations.

Several papers calculate exposure originating from specific sources [11], [12], [13], [14] where some convert the uplink (UL) radiation into localized SAR for head and torso [13], [14]. With the advent of 5G, paper [15] describes how the localized SAR-values are achieved from all different sources. Finally, [16] describes how the electronic radiation can be converted into whole body SAR values.

In a realistic network, some users are calling while others are using other types of telecommunication services like browsing the web. Therefore, all absorbed electromagnetic exposure should be expressed in whole body SAR while still covering all sources.

B. Optimized UAV-aided networks

A UAV knows several applications. It was originally mainly used to support the military for surveillance and remote attacks without endangering pilots [17]. However, UAVs have recently become more accessible by the general public due to decreasing costs. This allowed UAVs to be researched for various applications.

A UAV equipped with a femtocell base station antenna is called a Unmanned Arial Base Station (UABS) which brings several advantages like mobility and rapid deployment. However, it brings also challenges like limited weight of the payload and sparse power supply.

Kawamoto et al. introduced in [18] a WiFi network with the support of UAVs while considering resource allocation and antenna directivity. Gangula et al. illustrates in [19] how UAVs can be used as a relay for Long-Term Evolution (LTE) and Zeng et al. proposes in [17] a tutorial in 5G-and-beyond wireless systems where challenges like energy consumption, mobility and antenna direction are discussed. In [20], Deruyck et al. designed a capacity based deployment tool for UAV-aided emergency networks for large-scale disaster scenarios where an ideal flying height of 100 m is suggested. This was expanded in [21] with a performance evaluation of the direct-link backhaul of this tool where a slightly lower flying height of 80 metres is recommended.

Mozaffari et al. provides in [22] guidelines on how to optimize and analyse UAVs equipped for wireless communication equipment. A research area that has been excessively studied is the location solution optimization problem where networks are designed in such a way that certain goals like minimal power consumption or shortest flying distance are achieved [23], [24], [25], [26]. These optimizations can be done through different implementation methods like exact algorithms or machine learning [22], [27].

Research where network is optimized towards electromagnetic exposure is rather limited. Deruyck et al. discusses in [12] how a terrestrial network can be optimized towards either a minimal exposure or minimal power consumption of the entire network. However, to the best of the author knowledge, no research has been done where a UABS-network has been optimized towards electromagnetic exposure.

C. Technologies

For the deployment of the network, the more robust UAV from [20] will be used (details in table III) and will be operating in the 2.6 GHz bandwidth. Since the users are assumed to experience a constant electromagnetic exposure without interruptions, frequency division duplex is used.

The onboard antenna of the UAV will act as the gateway between the UE and the backhaul network. However, determining which antenna to use and how to position it, can be challenging. The radiation pattern from the antenna can be influenced by the UAV [28]. Also the fact that the UAV will hover above the user makes traditional 2D modelling insufficient. A 3D-model which accounts for both elevation and azimuth directivity will be required [17].

The easiest radiation pattern is a hypothetical isotropic radiator which radiates equally in all directions. Antennae that radiate equal quantities for a certain plane are called omnidirectional antennae [17] and several UABSs use antennae like monopoles, dipoles and wing antennae [29], [30], [31], [32]. Another type of antennae are directional antennae which save energy by focussing the electromagnetic energy where it is needed. One type that has excessively been researched in various array-configurations is a microstrip patch antenna [33], [34], [35]. These provide several advantages compared to traditional antennae [36], [37] like lightweightness and being low in cost, causing them to be more aerodynamic.

A basic microstrip antenna consists of a ground plane and a radiating patch, both separated by a dielectric sub-

strate. Several variations exist like microstrip patch antennae, microstrip slot antennae and printed dipole antennae which all have similar characteristics [36], [37]. They all are thin, support dual frequency operation and they all have the disadvantage that they will transmit at frequencies outside the aimed band which is also known as spurious radiation. The microstrip patch and slot antenna support both linear and circular polarization while the printed dipole only supports linear polarization. Further, the fabrication of a microstrip patch antenna is considered to be the easiest of the considered patch antennae [36].

Fig. 1 shows a microstrip patch antenna made of Teflon and an aluminium patch. The antenna is attached to a UAV and is pointing towards the ground where the users are located.

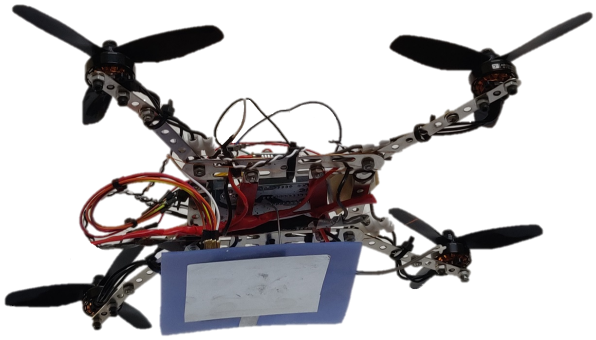

Fig. 1: Image of a microstrip patch antenna attached to the bottom of a UAV.

III. Methodology

The first subsection explains how electromagnetic radiation is calculated for each source and how to convert these values to SAR. The second subsection gives a overview of how a microstrip patch antenna can be designed. The third section discusses how the network can be optimized towards either electromagnetic exposure or power consumption and finally the algorithm itself is explained.

A. Electromagnetic Exposure

A.1 Total Electromagnetic Exposure

The total whole body SAR ($SAR_{10g}^{wb,total}$) of a user can be calculated by a simple sum of individual SAR values from the different sources and is based on [15]. This formula assumes that the users are holding their device next to their ear and therefore investigates localized SAR for head and torso area. However for this case, this would result into incorrect conclusions since the position of the device relative to the user is unknown. The position of the phone can be next to the head but also in front of the user. The induced electromagnetic radiation will therefore be expressed in function of the entire body.

$$SAR_{10g}^{wb,total} = SAR_{10g}^{wb,myUE} + SAR_{10g}^{wb,myUABS} + SAR_{10g}^{wb,otherUE} + SAR_{10g}^{wb,otherUABSs} \quad (1)$$

The first parameter, $SAR_{10g}^{wb,myUE}$, indicates the absorbed electromagnetic radiation by the whole body originating from the user's own device. Despite that the UL radiation is destined for the serving UABS, a portion of that radiation is directly absorbed by its user, due to the omnidirectional nature of the mobile's antenna. The second parameter, $SAR_{10g}^{wb,myUABS}$, represents the downlink (DL) radiation caused by the UABS that is serving the user. As the third parameter, we have the $SAR_{10g}^{wb,otherUE}$ which is radiation caused by other people's devices. The radiation of these devices is once again destined for a specific UABS but again, a portion of that UL radiation will also be absorbed by our user. Finally, $SAR_{10g}^{wb,otherUABSs}$ represents the DL radiation by the other UABSs to which our user is exposed to but not served by. An illustration is given in fig. 2. The green arrow stands for near-field radiation, the others represent far-field radiation.

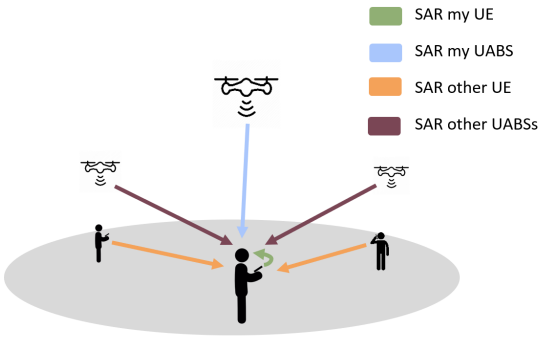

Fig. 2: Illustration of the network that shows how the average user (here shown in the center) is influenced by different types of sources.

A.2 Electromagnetic Radiation from a Single Source

In order to find the total electromagnetic radiation to which a user is exposed, the electromagnetic radiation from each sources needs to be calculated first. This is done with formula 2 which applies to all sources in the far-field. This includes all UABSs and all User Equipment (UE) belonging to other people. The exposure E of a single user u from a single radiator i can be calculated as follows.

$$E_i(u)[V/m] = 10^{\frac{RRP(u)[dBm]-43.15+20*\log(f[MHz])-PL(u)[dB]}{20}} \quad (2)$$

Calculating the real radiation power (RRP) for a certain user u, requires first the equivalent isotropic radiation power (EIRP)-value to be calculated [11], [12]. This is achieved by adding the transmission power P_{tx} to the transmitter gain G_t and thereafter subtracting the feeder loss L_t. This formula needs to be expanded to also account for attenuation from the used antenna. This value depends on the angle between this user and the antenna's main beam. The attenuation from an equivalent isotropic radiator is always zero. This leads to the following formula.

$$RRP[dBm] = P_{tx}[dBm] + G_t[dBi] - L_t[dB] \\ -attenuation(u)[dB] \quad (3)$$

The used frequency in formula 2 is denoted as f and is expressed in MHz. Since LTE is used, this value will be 2600 MHz.

At last, formula 2 requires the path loss PL. In order to calculate this, an appropriate propagation model — of which several exist— is required. The Walfish-Ikegami model is used since it performs well for femtocell networks in urban areas [20].

A.3 Combining Exposure

The total electromagnetic exposure E_{tot}, in a certain spot, originating from different sources can be calculated with formula 4. E_i stands for the electromagnetic exposure from source i and n stands for all far-field radiators of a certain category which will either be UABSs or UE from other people. E_{tot} will be calculated for each location where a user is positioned.

$$E_{tot}[V/m] = \sqrt{\sum_{i=1}^{n}(E_i[V/m])^2} \quad (4)$$

A.4 Converting electromagnetic radiation into SAR-values

Formula 1 expects that the radiation is expressed in whole body SAR-values. To make this calculation possible, a distinction has to be made between near-field SAR ($SAR^{wb,nf}$) and far-field SAR ($SAR^{wb,ff}$). $SAR_{10g}^{wb,myUE}$ is a form of near-field radiation, all the other types are far-field radiation.

Converting the electromagnetic radiation is done with a conversion factor which is based on Duke of the Virtual Family. Duke is a 34-year old male with a weight of 72 kg, a height of 1.74 m and BMI of 23.1 kg/m [16]. Research shows that the conversion factors for WiFi in the far-field is $0.0028\frac{W/kg}{W/m^2}$ and $0.0070\ \frac{W/kg}{W}$ for the near-field [16]. Since WiFi, at a frequency of 2400 MHz, is very close to LTE, at 2600 MHz, it is assumed in [16] that this value is also applicable for LTE. Calculating SAR from far-field radiation is done as follows:

$$S[W/m^2] = \frac{(E_{tot}[V/m])^2}{337} \quad (5)$$

$$SAR_{10g}^{wb,ff}[W/kg] = S[W/m^2] * 0.0028 \left[\frac{W/kg}{W/m^2}\right] \quad (6)$$

The constant in equation 6 converts the power flux density S to the required $SAR_{10g}^{ff,wb}$. To make this possible, the electromagnetic radiation from formula 4 should first be converted to the power flux density with formula 5.

The SAR caused by near-field radiation is calculated by multiplying the constant with the used transmission power P_{tx} of the UE which results in the following formula:

$$SAR_{10g}^{wb,nf}[W/kg] = 0.0070 \left[\frac{W/kg}{W}\right] * P_{tx}[W] \quad (7)$$

The power of the UE can be calculated using equation 8 [16].

$$P_{tx}^{UE} = min\{P_{max}[dBm], \\ P_{pusch}[dBm] + \alpha * PL[dB] + 10log(M) + \sigma\} \quad (8)$$

P_{max} is the maximum allowed transmission power by UE for LTE, defined at 23 dBm. However, this is the worst case and the actual used power is usually much lower thanks to power control. P_{pusch} is the required received power at the UABS and will here be -120 dBm. α is the path loss compensation factor set to one which means full compensation [38], [39]. For the 20-MHz channel used in this paper, M will be set to 100 and σ, as the correction factor, is set to zero [16], [38].

B. Microstrip Patch antenna

A microstrip patch antenna is chosen because it allows easy production but more important, it has a low weight and has a thin profile causing it to be very aerodynamic which is useful when attaching it to a drone [36].

The dimensions of the antenna depend on the frequency it is operating at and the characteristics of the used substrate. The antenna will be radiating at a centre frequency f_0 of 2.6 GHz. Each substrate has a dielectric constant ϵ_r representing the permittivity of the substrate that depends on the used material. Substrates with a high dielectric constant and low height reduce the dimensions of the antenna while a lower dielectric constant with a high height improves the performance of the antenna [37], [40]. In this research, a substrate like glass is chosen because of the higher dielectric constant of $\epsilon_r = 4.4$ compared to materials like Teflon with only a dielectric constant of $\epsilon_r = 2.2$ [37]. Doing this in combination with an antenna height of 2.87 mm will decrease the dimensions of the entire antenna surface. This comes in handy since UAVs only have limited space available.

Description	Symbol	Value
Center frequency	f_0	2600 MHz
Dielectric constant	ϵ_r	4.4
Height of the substrate	h	0.00287 m

TABLE II: Overview of configuration parameters.

The dimensions of the radiating patch can be calculated with the formulas from [37], [40]. Doing so will result in a radiating patch of 35.09 mm by 26.55 mm and a groundplane of at least 52.40 mm by 43.80 mm. The microstrip patch antenna as illustrated in fig. 3 will result in the radiation pattern of fig. 4.

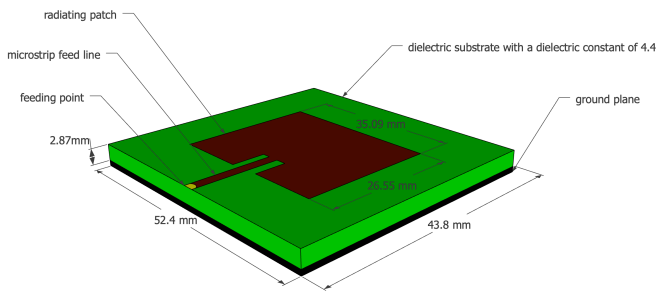

Fig. 3: Design of the microstrip patch antenna.

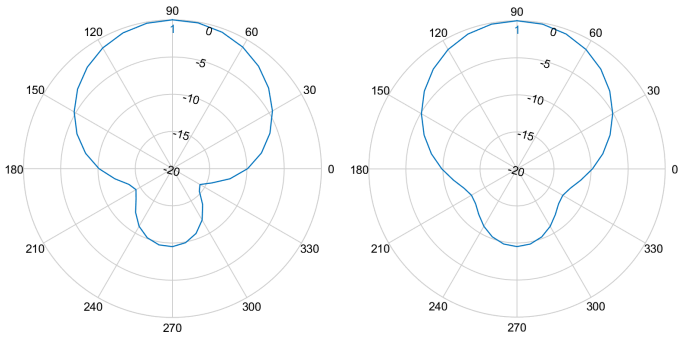

(a) E-plane (b) H-plane

Fig. 4: Radiation patterns generated by the used microstrip patch antenna.

C. Optimizing the network

Deruyck et al. discusses in [12] how a terrestrial telecommunication network either can be optimized towards electromagnetic exposure of an individual or towards power consumption of the entire network. However, an increasing transmission power of an antenna comes with an increasing electromagnetic exposure. This is not the case considering both values for an entire network. In fact, the authors from [12] prove that both become inversely equivalent. The reason why the network behaves like this is because it is often cheaper to increase the exposure of an already active base station than activating a new one. This leads to the following fitness function which is based on [12].

$$f = w * \left(1 - \frac{E_m}{E_{max}}\right) + (1 - w) * \left(1 - \frac{P}{P_{max}}\right) * 100 \quad (9)$$

Formula 9 returns a fitness value which represents the performance of the entire network. w is the importance factor of electromagnetic exposure ranging from 0 to 1, boundaries included. A w set to 0 means that electromagnetic exposure is not important. Such network will therefore be called a power consuption optimized (PwrC. Opt.) network. Likewise, a w set to 1 means that minimizing exposure is top priority and will result in an exposure optimized (Exp. Opt.) network. P_{max} is the power consumption of all UABSs, both active and inactive, when radiating at the highest level possible while P is the effective power used by the current designed network. This will be the power required for the flying UAVs themselves and their antennae. E_m will be the weighted exposure of the average user for the current designed network and E_{max} the weighted average of the electromagnetic exposure when all antennae are at their highest power level.

When optimizing the network, it is not only important to consider the average exposure of all users, but also to limit high extremes [12]. A weighted average will be used not only considering the median but also the 95 percentile from all users' DL exposure using formula 10. Since both values are considered to have equal importance, the weight factors w_1 and w_2 will both have an equal importance of 50%.

$$E_m = \frac{w_1 * E_{50} + w_2 * E_{95}}{w_1 + w_2} \quad (10)$$

D. Simulation Tool

D.1 Main Algorithm

First, a description of the area has to be provided to the tool. This is done with so-called shape-files. These files contain a complete description about the shape of the buildings. Thereafter, users are uniformly distributed over the area and a temporary UABS is positioned above each user. Now, the decision algorithm needs to decide which of these UABSs can actually remain and how strong each one should be radiating. Once the decision algorithm is done, the tool checks whether the number of online UABSs does not acceed the capacity of the facility where the UABSs are stored. If this is the case, the UABSs covering the least amount of users will be removed.

D.2 Decision Algorithm

Solving the network is done by the decision algorithm and starts by calculating the path loss between all users and between users and UABSs. Thereafter, the algorithm iterates over each user and tries to connect that user to each UABS. This connection is not always possible. A UABS might be saturated with users and will not be able to cover yet another one or maybe the user is so far away that in order to cover that user, the UABS would have to exceed its maximum allowed input power. If however a connection is possible, the user will be connected to that UABS and the fitness function (eq. 9) is applied. This is repeated for each UABS. Only the connection which results in the best fitness value for the entire network will be used. Doing so will make sure that, given the currently designed network, the user is optimized. In other words, each user is optimized and not the entire network. It is however assumed that the average network will be optimized as well. Thereafter, the tool shifts to the next user. When the last user has been processed, the network is fully designed for an unlimited number of UAVs and the result is returned to the main algorithm for further processing. The flowchart of this algorithm is given in fig. 5.

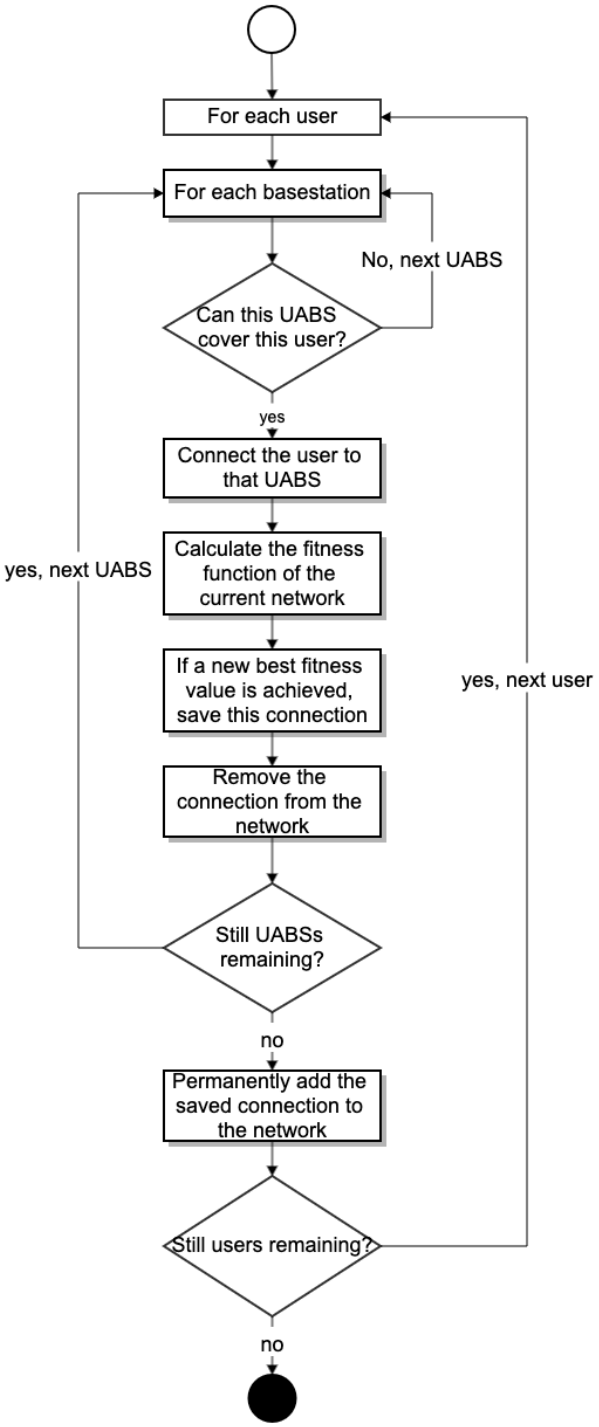

Fig. 5: Flowchart of the decision algorithm.

IV. Scenarios

The default configuration is given in table III and is applicable in all scenarios unless mentioned otherwise in the restrictions of that specific scenario.

Three main scenarios will be investigated. The first one has only one user and one UABS present in the network. SAR, electromagnetic exposure, power consumption and antenna transmission power are investigated at different flying heights.

Broadband cellular network	
Technology	LTE
Frequency	2.6 GHz
Power offset (P_{pusch})	-120 dBm
Path loss compensation (α)	1
Correction value	0 dBm
Number of used resource blocks	100
Femtocell antenna	
Maximum P_{tx}	33 dBm
antenna direction	downwards (az: 0°; el: 90°)
Gain	4 dBm
Feeder loss	2 dBm
Implementation loss	0 dBm
radiation pattern	EIRP or microstrip patch
Flying altitude	100 m
UAV	
UAV power	13.0 A
Average UAV speed	12.0 m/s
Average UAV power usage	17.33 Ah
UAV battery voltage	22.2 V
UE Antenna	
Height	1.5m from the floor
Gain	0 dBm
Feeder loss	0 dBm
Radiation pattern	EIRP
Quantity in network	224

TABLE III: Overview of default configuration values.

In a second scenario, the network is expanded for multiple users while still considering only one UABS. Two parameters will be evaluated. The first one will be a variable flying height ranging from 20 to 200 metres with a fixed number of 224 users. This is the average population size on an usual day at 5 p.m. in Ghent [20]. The second evaluated parameter is the number of users ranging from 50 to 600 users while flying height is set to 100 metres [20]. The power consumption, electromagnetic exposure and specific absorption rate are investigated for each parameter.

The third scenario is quite similar to the previous scenario. The same two parameters are investigated, but now an unlimited number of UABSs is available.

Four configurations are considered for each evaluated parameter in each scenario. There are two possible antennae, namely EIRP and microstrip patch antenna, which can both be applied in a PwrC. Opt. network or an Exp. Opt. network. An overview of the simulation configuration scenarios is presented in fig. 6

It is important to note that all measured values are strictly limited to the sources mentioned in the previous section and thus only cover data traffic between UE and UABSs. Any other potential sources like backhaul links or any other technology will not be covered.

		Optimization strategy	
		Exposure optimized	Power consumption optimized
Antenna type	Equivalent isotropic radiator	EIRP Exp Opt	EIRP PwrC Opt
	Microstrip patch antenna	Microstrip Exp Opt	Microstrip PwrC Opt

Fig. 6: Matrix with the four possible configurations

V. Results

Four configurations will be investigated while evaluating two parameter, being the population size and flying height. The parameters are evaluated for three different scenarios by monitoring the power consumption, electromagnetic exposure and SAR-values. The electromagnetic radiation and SAR are measured for the weighted average user using equation 10 with both w_1 and w_2 set to 50%. Each result is averaged over 20 simulations.

A. One User and One UABS

The results show that for a varying flying height, a logarithmic relationship exists between the P_{tx} and the flying height. This is mainly caused by the logarithmic scale in which the decibels of the P_{tx} are expressed. Each time the flying height becomes too large to cover, the P_{tx} increases with one dBm. When using the default configuration, with a maximum P_{tx} of 33 dBm, a UABS can fly up to 387 m before losing connection in a free line of sight (LoS) scenario.

This scenario is investigated with a microstrip patch antenna using power consumption optimization. However, the chosen optimization strategy does not really matter because the decision algorithm decides which user needs to be connected to which UABS. Since only one UABS is available, both optimization strategies will behave identical. Further, the used antenna will not make any difference. The user is positioned in the perfect centre of the main beam where there is no attenuation experienced for both antennae.

When investigating this scenario at different flying heights, it is noticed that the UL radiation increases exponentially while the DL radiation remains constant at 10 nW/kg during the entire time as shown in fig. 7. The reason that the DL radiation remains constant is because of the power control which makes sure that no more power is used than strictly necessary. We can therefore confirm that the electromagnetic exposure is a constant fraction of power and distance. The UL radiation starts very low at 1 nW/kg but surpasses the DL radiation around 80 metres.

B. Increased Population with one UABS

B.1 Variable Flying Height

A PwrC. Opt. network has higher exposure compared to an Exp. Opt. network; a behaviour that was already proven by [12]. However, for this scenario, a PwrC. Opt.

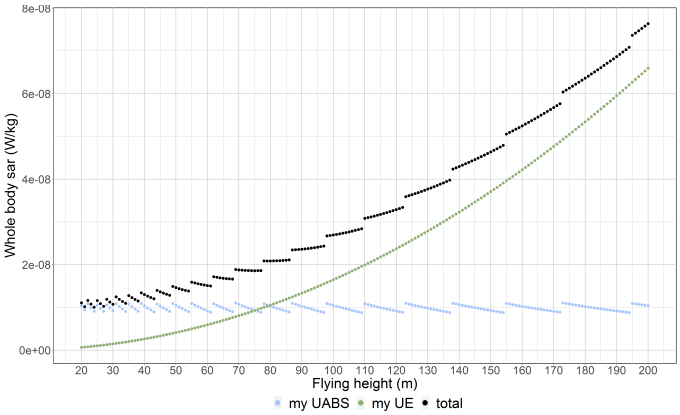

Fig. 7: This figure shows how SAR values from different sources are influenced by different flying altitudes.

network will not necessarily result in a lower power consumption. For example, at 100 metres, an EIRP Exp. Opt. network exposes the average user to 1.5 mV/m less but requires 20 mW more. To understand this, the behaviour of the deployment tool needs to be understood first. A PwrC. Opt. network will result in a few high powered UABSs because increasing the input power of an antenna costs less than activating a new UAV. Likewise, an Exp. Opt. network generates a lot of low powered UABSs because the lower the power of the antenna, the lower the exposure. This has the consequence that the cover radius is less and therefore requires more UAVs which costs more energy. When only a limited amount of UABSs are available, like only one in this scenario, the tool will only keep UABSs which cover the most users. Since the power consumption of an individual UABS is higher in a PwrC. Opt. network and only one UABS remains in each configuration, the power consumption in a PwrC. Opt. network is often higher.

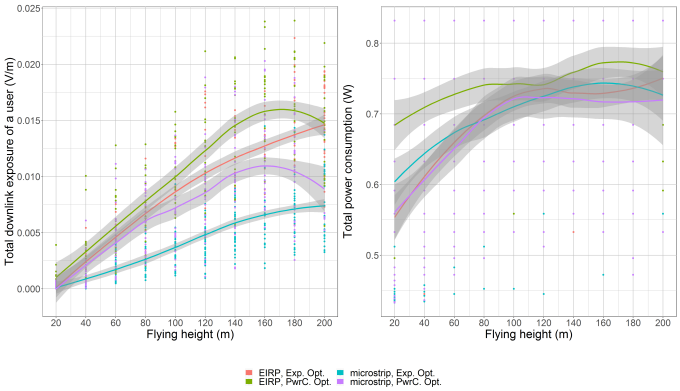

Fig. 8: Fig. (a) show how the flying height influences the downlink electromagnetic radiation of the average user and fig. (b) the power consumption of the entire network for the only UABS available in the network.

Further, fig. 8 also show that the exposure increases with higher flying altitudes because there is a lower probability

of having non line of sight (NLoS) links by obstructing buildings. This has as consequence that more users become covered. Increasing the flying height from 20 to 100 metres improves the coverage between 1% and 2% for all four configurations. The increasing electromagnetic radiation is however not unlimited. A microstrip PwrC. Opt. network is at his highest point around 162 metres and an EIRP PwrC. Opt. is at his highest at 195 metres. This decline starts later for exposure optimized networks and is situated outside the investigated flying range. The decreasing electromagnetic radiation at high flying altitudes is not caused by the obstructing buildings but by the distance in general.

Fig. 9 shows the whole body SAR_{10g} for the weighted average user, deducted from all electromagnetic sources. When investigating the three different sources, we see that the SAR^{myUABS} shows the same curve as it did with the electromagnetic exposure in fig. 8.a. This is normal behaviour considering that equation 6 is able of converting the DL exposure to SAR by simply multiplying with a constant. During the entire time, SAR^{myUABS} is the most dominant factor followed by the near-field radiation from the user's own device. The far-field radiation from other UE barely has influence. As an illustration, when the UABS flies at 140 metres, the average user in an EIRP PwrC. Opt. network will experience around 2.1 nW/kg from the UABS and around 0.2 nW/kg from his own device. The exposure from other UE can be neglected with 0.03 pW/kg. A low but plausible value considering that most UE are not radiating anything since they are uncovered.

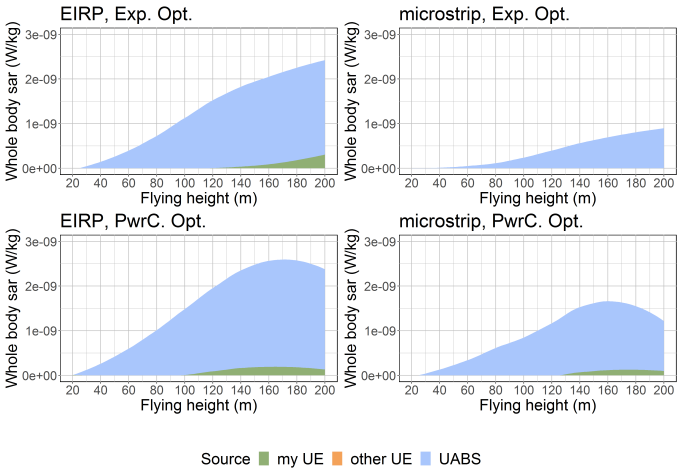

Fig. 9: Influence of the flying height for each considered configuration.

B.2 Variable Number of Users

The number of users present in the network increases from 50 to 600. Fig. 10.b shows that the number of covered users increases linearly compared to the number of users present in the network. It illustrates how an equivalent isotropic radiator is able to reach more users compared to a microstrip patch antenna. Just like an power consumption optimized network is able to reach more users than an exposure optimized network.

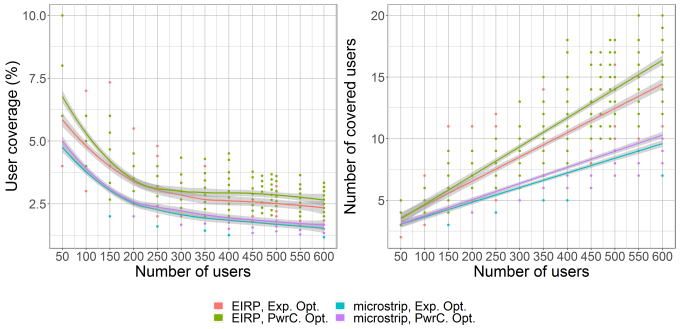

Fig. 10: The influence of increasing traffic on the user coverage.

For example, with 600 users, 5 to 7 additional people can be covered when replacing a microstrip patch antenna with an equivalent isotropic radiator and changing an exposure optimized network with an power consumption optimized network will cover one or two additional users.

Fig. 11.a gives the electromagnetic exposure of the weighted average user for different populations sizes while 11.b presents the power consumption of the entire network for all these population sizes. Figure 11.a is influenced by 10.a. When less users are covered, the exposure of the average user will decrease as well. For example, in an EIRP PwrC. Opt. network, 50 users have a 6.75% coverage which corresponds with a weighted average exposure of 18 mV/m while 600 users with 2.75% coverage only have 9 mV/m. Further, fig. 11.b is directly influence by fig. 10.b. When the UABS has to cover more users, the probability that some of these users have a worse path loss is higher. The UABS solves this problem by increasing the power consumption. Increasing the population from 50 to 600 will require between 0.05 and 0.1 W more. For this scenario, no clear difference in power consumption exists between the four configurations.

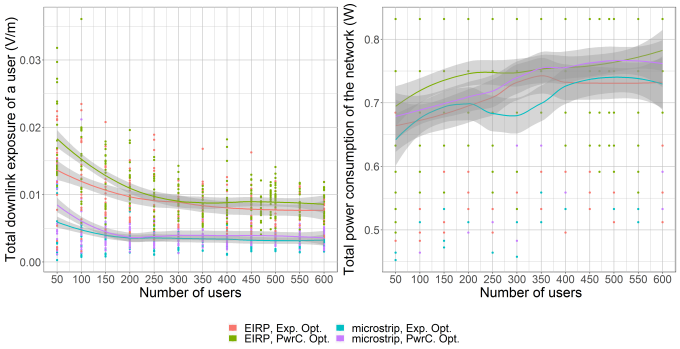

Fig. 11: These two figures show how various sizes of population influence the downlink electromagnetic radiation of the average user (left) and power consumption of the entire network (rights) for one UABS available in the network.

The SAR coming from the users own device is on average zero since most users are uncovered. Fig. 12 shows the exposure for the covered user just below the UABS. Scenario I already showed that the SAR from the user's own device is only influenced by the flying height and is also confirmed by the results in fig. 12.a where constant SAR^{myUE} is measured of 0.15 $\mu W/kg$. The SAR from the UABS experiences a slight increase of 0.005 $\mu W/kg$.

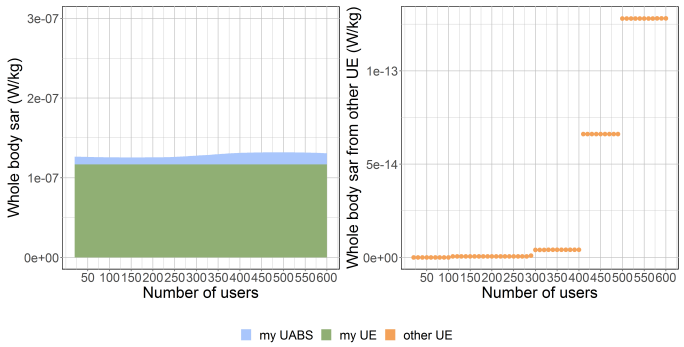

Fig. 12: SAR-values for the user who is directly beneath the only UABS available.

When the population grows, more users will be near the UABS. The UABS will likely decide to cover these users as well as visible in fig. 13. These users might have a slightly worse path loss because of obstructing buildings or somewhat bigger distance. The UABS reacts to this by increasing his power consumption causing an increase in the DL SAR for the central user. The far-field radiation from UE is very low as mentioned before and therefore added separately in fig. 12.b. It shows that the SAR from other UE increases from zero to 0.15 pW/kg.

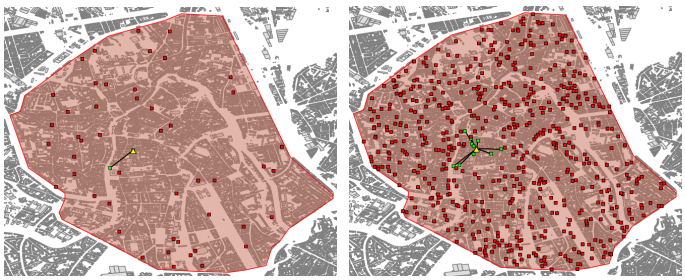

(a) 50 users (b) 600 users

Fig. 13: Overview of which users are connected to the UABS.

C. Unlimited Number of UABSs

C.1 Variable Flying Height

The same scenario as in the previous section is investigated. Only now, an unlimited number of UABSs is available. The results prove that the different optimization strategies work as intended. A PwrC. Opt. network has indeed a lower power consumption and therefore result in higher electromagnetic radiation. On the other hand, an Exp. Opt. network will reduce the electromagnetic exposure by using more UAVs and hence increase the network's power consumption. This conclusion was already made in [12] and is supported by these results. For example, when comparing both optimization strategies for the same equivalent isotropic radiator and the same default flying height, we see that the power consumption optimized network requires 51 W and therefore exposes its users to 15 mV/m. When optimizing towards electromagnetic radiation, the exposure drops to 11.5 mV/m but at a cost of a higher power consumption of 54 W.

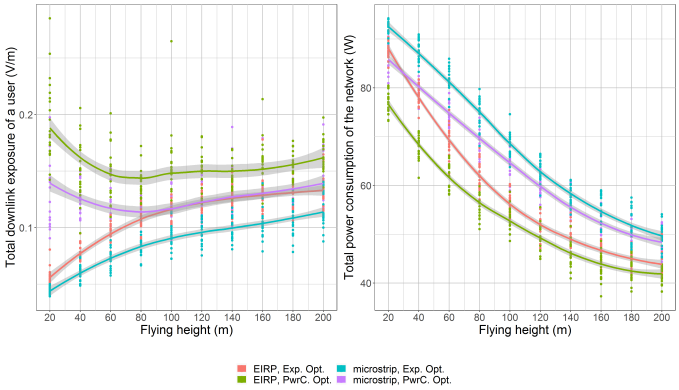

Fig. 14: These two figures show how the flying height influences the downlink electromagnetic radiation of the average user (left) and power consumption of the entire network (right) for an unlimited number of UAVs.

The exposure in fig. 14 shows that an Exp. Opt. network increases logarithmically while the PwrC. Opt. network rather has a concave relationship with the flying height, and has its lowest point at around 70 metres.

Fig. 15.a shows that the optimal coverage is achieved at a low flying height of 40 metres with around 99% coverage. However, there is a downside to this. Fig. 15.b shows that the number of required UAVs increases when the flying altitude becomes lower; a behaviour which was also determined in [20]. For example, an microstrip Exp. Opt. network and an EIRP PwrC. Opt. network require respectively 84 and 64 UABSs at a flying altitude of 200 m which increases respectively to 211 and 162 UABSs at a much lower flying altitude of 20 m.

Fig. 16 shows how each source contributes to the total SAR. A first consequence of raising the flying altitude from 20 to 200 metres is an increase between 89 and 141 nW/kg for SAR originating the user's own device; a behaviour also explained in the first scenario. Fig. 16 shows that once the flying altitude surpasses the NLoS of the buildings, around 70 to 80 metres, the SAR^{myUABS} remains more or less constant for all configurations. This is situated around 160 nW/kg for microstrip PwrC. Opt. networks. The microstrip Exp. Opt. and EIRP PwrC. Opt. networks has on average 98 nW/kg and the EIRP Exp. Opt. network is situated around 47 nW/kg. These higher flying altitudes will also result in an increase in electromagnetic radiation

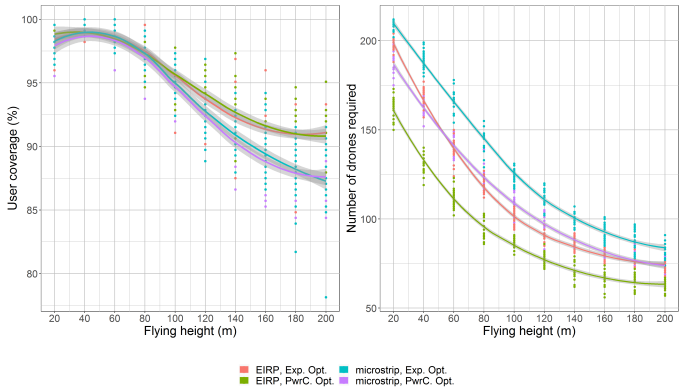

Fig. 15: This graph shows how much UAVs are required at different flying heights while trying to achieve a 100% coverage.

from other UABSs. Raising the flying altitude from 20 to 200 metres will increase the the $SAR^{otherUABS}$ between 115 and 140 nW/kg for EIRP antennae and between 54 and 74 nW/kg for microstrip patch antennae for both optimization strategies.

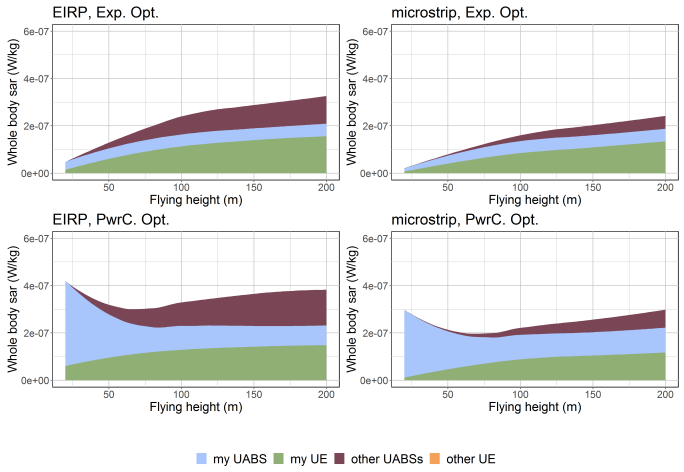

Fig. 16: Each chart corresponds with one of the four possible configurations. The contribution of each source towards the total SAR for a varying flying height is shown.

C.2 Variable Number of Users

The second evaluated parameter of this scenario is a variable number of users while the flying height is fixed to 100 metres. Fig. 17.a shows how the deployment tool tries to reach a 100% coverage. The percentage of covered users is slightly less for smaller networks. For only 50 users, an average coverage of around 93% is achieved while a network with 600 users has a coverage of around 97%. Fig. 17.b prove that more UAVs are required for these large populations. The difference in optimization strategy is very little for a small amount of people but increases very quickly. When the population increases from 50 to 600 users, 200 more UABSs are required by a microstrip Exp. Opt. network, around 130 more UABSs for an EIRP Exp. Opt. network or a microstrip PwrC. Opt. network and 110 more UABSs for an EIRP PwrC. Opt. network. This is an expected behaviour when looking at scenario II, the percentage of covered users decreases for these larger populations.

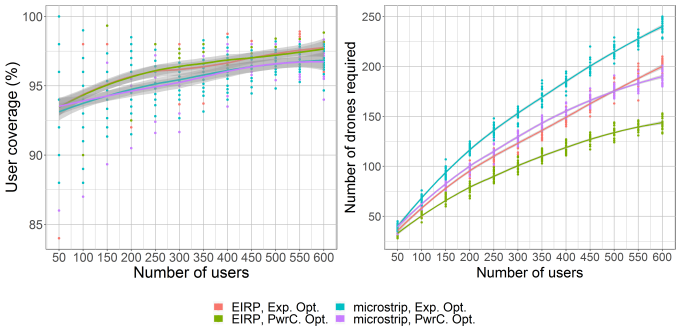

Fig. 17: This graph shows how much UAVs are required for different flying heights while trying to achieve a 100% coverage.

Fig. 18 shows that the electromagnetic radiation and power consumption increase for larger populations which is normal since more UABSs will be available. When the population increases from 50 to 600 users, the electromagnetic radiation increases between 80 and 130 mV/m depending on the configuration. The power consumption with 50 users is for all configurations around 20 W. Once the population is increased to 600 users, a microstrip Exp. Opt. network will require 130 W, a microstrip PwrC. Opt. network requires 117 W, EIRP Exp. Opt. networks require 107 W and EIRP PwrC. Opt. network requires 92 W.

The correct behaviour of the decision algorithm became already clear in the previous subsection but is also confirmed here. When comparing both optimization strategies, a power consumption optimized network requires around 5 W less but exposes its users between 27 mV/m and 30 mV/m more than exposure optimized networks. Further, it is also noticed that equivalent isotropic radiators cause more electromagnetic radiation for less energy compared to microstrip patch antennae. When comparing the two types of antennae for a default number of 224 users, an equivalent isotropic radiator will expose the average user between 25 mV/m and 27 mV/m more while requiring around 12 W less than when the network would be using a microstrip patch antennae.

Fig. 19 represents the SAR from the weighted average user and shows how the SAR coming from the user's own device remains almost constant. The flying altitude is always the same so also the required energy to cover that distance will remain the same. For both optimization strategies, the SAR^{myUE} for networks with equivalent isotropic radiators vary around 1.1 $\mu W/kg$ and around 0.7 $\mu W/kg$ for networks using microstrip patch antennae. The SAR^{myUABS} barely increases in an exposure optimized network and is situated around 0.5 $\mu W/kg$ for both antennae. The power consumption optimized network also

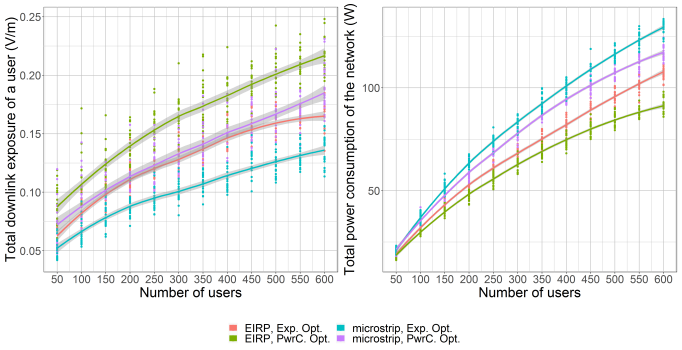

Fig. 18: The influence of the population size on the downlink electromagnetic radiation (a) and power consumption (b).

starts around 0.5 $\mu W/kg$ but increases when more users become online. A normal behaviour when considering that these UABSs try to cover much more users. Therefore, the SAR^{myUABS} with 600 users increases up to 1 $\mu W/kg$ for an equivalent isotropic radiator and almost 2 $\mu W/kg$ for a microstrip patch antenna. The SAR value that increases the most is $SAR^{otherUABS}$ which starts really low with less than 0.1 $\mu W/kg$ for 50 users for all configurations. The SAR increases however very fast. The biggest increase is noticed in an EIRP PwrC. Opt. network where 3 $\mu W/kg$ is measured for 600 users. The $SAR^{otherUE}$ increases the least for microstrip Exp. Opt. with only 1 $\mu W/kg$ for 600 users.

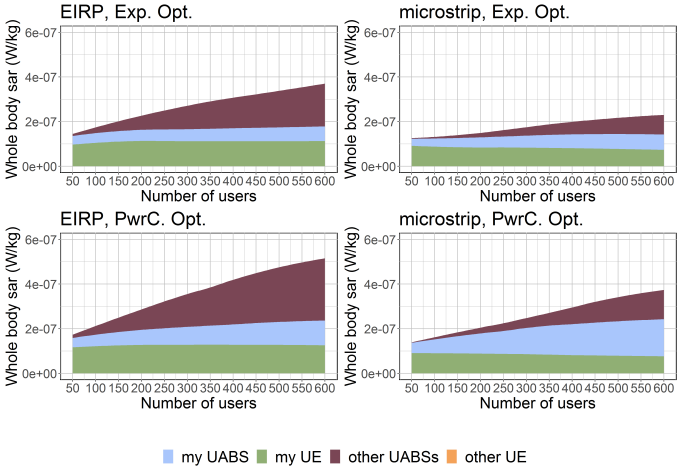

Fig. 19: Each figure corresponds with a certain configuration and shows how the SAR from different sources are influenced by an increasing population size. An unlimited number of UABSs is available.

VI. Conclusion

A capacity-based deployment tool has been used to identify the SAR of a user and how a network can be optimized towards DL electromagnetic exposure and overall power consumption. This has been investigated for different flying heights, number of users and number of available UABSs. The results confirm that optimizing towards electromagnetic exposure and total power consumption indeed result in conflicting requirements as it was already stated in [12]. The proposed fitness function works as intended. For default configurations, the electromagnetic field radiation from a power consumption optimized network can be reduced up to 23% for equivalent isotropic radiators and 30% for microstrip patch antennae by optimizing towards electromagnetic exposure. Doing so, decreases the range of the UABS and much more UABSs will be needed. Therefore, exposure optimized networks will, on average, use 18 UAVs more than power consumption optimized networks and require therefore 5 W more energy.

A directional microstrip patch antenna is introduced because it gives several advantages compared to omnidirectional antennae. Directional antennae are able to focus their energy there where it is needed, namely towards the ground. Microstrip patch antennae further benefit from their thin and lightweight design. A microstrip patch antenna with an aperture angle of 90° causes less electromagnetic exposure and coverage and requires more power compared to an equivalent isotropic radiator. For a default configuration, a microstrip patch antenna can reduce between 30% and 34% of the electromagnetic exposure emitted by an equivalent isotropic radiator. This will increase the power consumption with 11 W.

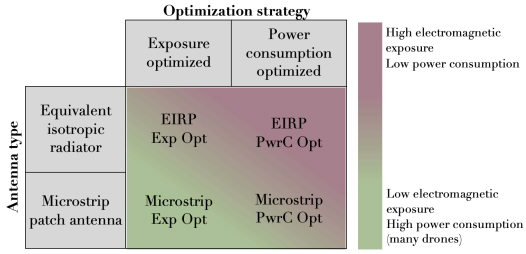

Fig. 20: Matrix with the four possible configurations, colour-coded based on the results.

Fig. 20 shows an overview based on the results from the two optimization strategies and the two types of antenna. Remarkable is that an EIRP exposure optimized network behaves very similar to a microstrip power consumption optimized network. Therefore, the microstrip patch antenna in a power consumption optimized network is recommended. The microstrip patch antenna will generate less electromagnetic radiation by design and the power consumption optimization reduces the number of required UAVs and power. A microstrip patch antenna with an aperture angle of 90° is considered as a good solution but if budget is more limited, an antenna with a larger aperture angle would further reduce cost without interfering with the Flemish legislation regarding electromagnetic exposure. The SAR from the configuration with the most exposure is still a hundred thousandth of the maximal allowed whole body SAR.

Fig. 21 gives an overview of the contribution of SAR in

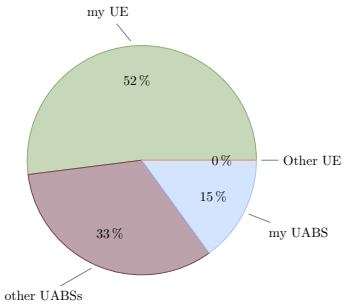

Fig. 21: Contribution from each source towards the total SAR that is experienced by the weighted average user. The percentages are averaged over the four considered configurations.

percentage to the total exposure for a default network. The values have been averaged over all four considered configurations. The user's main source of exposure is clearly the user's own device which contributes 52% of the total experienced exposure. A conclusion that was also made by the authors of [15] and [41]. Further, in [41] is also concluded that, thanks to power control, the electromagnetic radiation from the mobile phone comes really close to the exposure from the UABS. Also this is confirmed by the results. Fig. 21 shows that the electromagnetic exposure from all UABSs together covers the remaining 48% of which 15% is from the serving UABS. The electromagnetic exposure from devices belonging to other people can be ignored compared to the much higher electromagnetic exposure from the other sources and contributes only 0.0001%.

Further, the results show that power consumption and electromagnetic exposure increases when more users needs to be covered. When the population increases from 50 to 600 users, the electromagnetic radiation increases between 80 and 130 mV/m depending on the configuration. The power consumption increases with 110 W for all configurations. The main source that is influenced by the number of users is the SAR from other UABSs with an increase between 1 and 3 $\mu W/kg$, depending on the configuration. Further, increasing the flying altitude has a positive influence on the number of required UAVs which on their turn have a positive influence on power consumption. Increasing the flying altitude from 20 m to 200 m, decreases the number of required UAVs around 59%. This decrease was also noticed in [20]. Also authors from [15] made the conclusion that reduced path loss decreases electromagnetic exposure. The electromagnetic radiation from the UABSs remains more or less the same for flying altitudes between 80 and 200 metres. Most UABSs are in LoS and no more power will be used thanks to power control. However, the electromagnetic radiation from the user's own device does increase in order to reach the high flying UAVs. At around 80 metres, the exposure from the user's device surpasses the exposure from the serving UABS. When more UABSs are available in the network, electromagnetic exposure from other UABS will increase as well. This is because more UABSs come into LoS when the flying height becomes larger. Raising the flying altitude from 20 to 200 m will increase the SAR from other UABSs between 46 and 49 times when using an equivalent isotropic radiator antenna and between 70 and 85 times when using a microstrip patch antenna. When also considering the results from [21] where a flying altitude of 80 metres is suggested for an optimal access and backhaul connectivity, a flying height of 80 metres is also here proposed for the city centre of Ghent.

In conclusion, a microstrip patch antenna with an aperture angle of 90° is a suitable starting point for an antenna. This directional antenna focusses electromagnetic radiation where it is needed and unwanted sideways radiation is reduced. The sufficiently large aperture angle covers enough users. The antenna is recommended to be deployed in a power consumption optimized network since less UAVs are required and therefore also less expensive. The optimal flying height for the city centre of Ghent is believed to be situated at 80 metres since lower flying heights require much more UABSs and higher flying heights have a negative influence on the electromagnetic exposure.

As a future work, still some parameters require further evaluation. Different Physical Uplink Shared Channel (PUSCH) values are expected to have a big influence on UL radiation and exposure from backhaul connections still have to be considered. Further, MiMo and massive MiMo are ready to be supported since the tool can easily be extended with some more complex radiation patters like beamforming. Another consideration is improving the time complexity by replacing the exact algorithm with an heuristic algorithm.

Acknowledgement

Special thanks to the WAVES research group at Ghent University for providing access to their capacity based deployment tool and therefore making this research possible.

References

[1] "Base overschreed stralingsnormen na aanslagen," De standaard, 2016.

[2] L. Hardell and C. Sage, "Biological effects from electromagnetic field exposure and public exposure standards," Biomedicine and Pharmacotherapy, vol. 62, no. 2, pp. 104 – 109, 2008.

[3] "What are electromagnetic fields." https://www.who.int/peh-emf/about/WhatisEMF/en/index1.html. Accessed: 15-10-2019.

[4] "Elektromagnetische velden en gezondheid: Uw wegwijzer in het elektromagnetische landschap," Federale overheidsdienst: volksgezondheid, veiligheid van de voedselketen en leefmilieu, vol. 5, 2014.

[5] A. Ahlbom, U. Bergqvist, J. Bernhardt, J. Cesarini, M. Grandolfo, M. Hietanen, A. Mckinlay, M. Repacholi, D. H. Sliney, J. A. Stolwijk, et al., "Guidelines for limiting exposure to time-varying electric, magnetic, and electromagnetic fields (up to 300 ghz)," Health physics, vol. 74, no. 4, pp. 494–521, 1998.

[6] "Normen zendantennes." https://omgeving.vlaanderen.be/normen-zendantennes. Accessed: 19-03-2020.

[7] E. Commission, "Council recommendation of 12 july 1999 on the limitation of exposure of the general public to electromagnetic fields (0 hz to 300 ghz)," Official Journal of the European Communities, vol. 59, 1999.

[8] "Wireless devices." https://www.health.belgium.be/en/wireless-devices. Accessed: 13-05-2020.

[9] A.-K. Lee, S.-E. Hong, M. Taki, K. Wake, and H. Do Choi, "Comparison of different sar limits in sam phantom for mo-

bile phone exposure," in 2018 Asia-Pacific Microwave Conference (APMC), pp. 687–689, IEEE, 2018.

[10] W. H. Bailey, R. Bodemann, J. Bushberg, C.-K. Chou, R. Cleveland, A. Faraone, K. R. Foster, K. E. Gettman, K. Graf, T. Harrington, et al., "Synopsis of ieee std c95. 1™-2019 "ieee standard for safety levels with respect to human exposure to electric, magnetic, and electromagnetic fields, 0 hz to 300 ghz"," IEEE Access, vol. 7, pp. 171346–171356, 2019.

[11] D. Plets, W. Joseph, K. Vanhecke, and L. Martens, "Exposure optimization in indoor wireless networks by heuristic network planning," Progress In Electromagnetics Research, vol. 139, pp. 445–478, 01 2013.

[12] M. Deruyck, E. Tanghe, D. Plets, L. Martens, and W. Joseph, "Optimizing lte wireless access networks towards power consumption and electromagnetic exposure of human beings," Computer Networks, vol. 94, 12 2015.

[13] D. Plets, W. Joseph, S. Aerts, K. Vanhecke, G. Vermeeren, and L. Martens, "Prediction and comparison of downlink electric-field and uplink localised sar values for realistic indoor wireless planning," Radiation Protection Dosimetry, vol. 162, no. 4, pp. 487–498, 2014.

[14] D. Plets, W. Joseph, K. Vanhecke, and L. Martens, "Downlink electric-field and uplink sar prediction algorithm in indoor wireless network planner," in The 8th European Conference on Antennas and Propagation (EuCAP 2014), pp. 2457–2461, IEEE, 2014.

[15] S. Kuehn, S. Pfeifer, B. Kochali, and N. Kuster, "Modelling of total exposure in hypothetical 5g mobile networks for varied topologies and user scenarios," Final Report of Project CRR-816, Available on line at: https://tinyurl. com/r6z2gqn, 2019.

[16] D. Plets, W. Joseph, K. Vanhecke, G. Vermeeren, J. Wiart, S. Aerts, N. Varsier, and L. Martens, "Joint minimization of uplink and downlink whole-body exposure dose in indoor wireless networks," BioMed research international, vol. 2015, 2015.

[17] Y. Zeng, Q. Wu, and R. Zhang, "Accessing from the sky: A tutorial on uav communications for 5g and beyond," Proceedings of the IEEE, vol. 107, no. 12, pp. 2327–2375, 2019.

[18] Y. Kawamoto, H. Nishiyama, N. Kato, F. Ono, and R. Miura, "Toward future unmanned aerial vehicle networks: Architecture, resource allocation and field experiments," IEEE Wireless Communications, vol. 26, no. 1, pp. 94–99, 2018.

[19] R. Gangula, O. Esrafilian, D. Gesbert, C. Roux, F. Kaltenberger, and R. Knopp, "Flying rebots: First results on an autonomous uav-based lte relay using open airinterface," in 2018 IEEE 19th International Workshop on Signal Processing Advances in Wireless Communications (SPAWC), pp. 1–5, IEEE, 2018.

[20] M. Deruyck, J. Wyckmans, W. Joseph, and L. Martens, "Designing uav-aided emergency networks for large-scale disaster scenarios," EURASIP Journal on Wireless Communications and Networking, vol. 2018, 12 2018.

[21] G. Castellanos, M. Deruyck, L. Martens, and W. Joseph, "Performance evaluation of direct-link backhaul for uav-aided emergency networks," Sensors, vol. 19, no. 15, p. 3342, 2019.

[22] M. Mozaffari, W. Saad, M. Bennis, Y.-H. Nam, and M. Debbah, "A tutorial on uavs for wireless networks: Applications, challenges, and open problems," IEEE communications surveys & tutorials, vol. 21, no. 3, pp. 2334–2360, 2019.

[23] Q. Wu, L. Liu, and R. Zhang, "Fundamental trade-offs in communication and trajectory design for uav-enabled wireless network," IEEE Wireless Communications, vol. 26, no. 1, pp. 36–44, 2019.

[24] M. Deruyck, A. Marri, S. Mignardi, L. Martens, W. Joseph, and R. Verdone, "Performance evaluation of the dynamic trajectory design for an unmanned aerial base station in a single frequency network," in 2017 IEEE 28th Annual International Symposium on Personal, Indoor, and Mobile Radio Communications (PIMRC), pp. 1–7, IEEE, 2017.

[25] A. V. Savkin and H. Huang, "Deployment of unmanned aerial vehicle base stations for optimal quality of coverage," IEEE Wireless Communications Letters, vol. 8, no. 1, pp. 321–324, 2018.

[26] H. Huang and A. V. Savkin, "A method for optimized deployment of unmanned aerial vehicles for maximum coverage and minimum interference in cellular networks," IEEE Transactions on Industrial Informatics, vol. 15, no. 5, pp. 2638–2647, 2018.

[27] C. T. Cicek, H. Gultekin, B. Tavli, and H. Yanikomeroglu, "Uav base station location optimization for next generation wireless networks: Overview and future research directions," in 2019 1st International Conference on Unmanned Vehicle Systems-Oman (UVS), pp. 1–6, IEEE, 2019.

[28] A. Rizwan, D. Biswas, and V. Ramachandra, "Impact of uav structure on antenna radiation patterns at different frequencies," in 2017 IEEE International Conference on Antenna Innovations & Modern Technologies for Ground, Aircraft and Satellite Applications (iAIM), pp. 1–5, IEEE, 2017.

[29] M. Nosrati, A. Jafargholi, and N. Tavassolian, "A broadband blade dipole antenna for uav applications," in 2016 IEEE International Symposium on Antennas and Propagation (APSURSI), pp. 1777–1778, IEEE, 2016.

[30] M. Nosrati, A. Jafargholi, R. Pazoki, and N. Tavassolian, "Broadband slotted blade dipole antenna for airborne uav applications," IEEE Transactions on Antennas and Propagation, vol. 66, no. 8, pp. 3857–3864, 2018.

[31] B. A. Arand, R. Shamsaee, and B. Yektakhah, "Design and fabrication of a broadband blade monopole antenna operating in 30 mhz–600 mhz frequency band," in 2013 21st Iranian Conference on Electrical Engineering (ICEE), pp. 1–3, IEEE, 2013.

[32] L. Akhoondzadeh-Asl, J. Hill, J.-J. Laurin, and M. Riel, "Novel low profile wideband monopole antenna for avionics applications," IEEE transactions on antennas and propagation, vol. 61, no. 11, pp. 5766–5770, 2013.

[33] S. S. Siddiq, G. Karthikeya, T. Tanjavur, and N. Agnihotri, "Microstrip dual band millimeter-wave antenna array for uav applications," in 2016 21st International Conference on Microwave, Radar and Wireless Communications (MIKON), pp. 1–4, IEEE, 2016.

[34] Y. Zheng, J. Zhou, W. Wang, and M. Chen, "A low-profile broadband circularly polarized antenna array for uav ground-to-air communication," in 2018 IEEE Asia-Pacific Conference on Antennas and Propagation (APCAP), pp. 219–220, IEEE, 2018.

[35] X. Sun, R. Blázquez-García, A. García-Tejero, J. M. Fernández-González, M. Burgos-García, and M. Sierra-Castañer, "Circular array antenna tor uav-uav communications," in 2017 11th European Conference on Antennas and Propagation (EUCAP), pp. 2025–2028, IEEE, 2017.

[36] I. Singh and V. Tripathi, "Micro strip patch antenna and its applications: a survey," Int. J. Comp. Tech. Appl, vol. 2, no. 5, pp. 1595–1599, 2011.

[37] K. Kashwan, V. Rajeshkumar, T. Gunasekaran, and K. S. Kumar, "Design and characterization of pin fed microstrip patch antennae," in 2011 Eighth International Conference on Fuzzy Systems and Knowledge Discovery (FSKD), vol. 4, pp. 2258–2262, IEEE, 2011.

[38] R. Mullner, C. F. Ball, K. Ivanov, J. Lienhart, and P. Hric, "Contrasting open-loop and closed-loop power control performance in utran lte uplink by ue trace analysis," in 2009 IEEE International Conference on Communications, pp. 1–6, IEEE, 2009.

[39] M. Lauridsen, A. R. Jensen, and P. Mogensen, "Reducing lte uplink transmission energy by allocating resources," in 2011 IEEE Vehicular Technology Conference (VTC Fall), pp. 1–5, 2011.

[40] A. Sudarsan and A. Prabhu, "Design and development of microstrip patch antenna," International Journal of Antennas (JANT) Vol, vol. 3, 2017.

[41] A. Gati, E. Conil, M.-F. Wong, and J. Wiart, "Duality between uplink local and downlink whole-body exposures in operating networks," IEEE transactions on electromagnetic compatibility, vol. 52, no. 4, pp. 829–836, 2010.